Graphene-VP40 interactions and potential disruption of the Ebola virus matrix filaments

Jeevan B. GC[1], Rudramani Pokhrel[1], Nisha Bhattarai[1], Kristen A. Johnson[2], Bernard S. Gerstman[1,3], Robert V. Stahelin[2,4,5], Prem P. Chapagain[1,3]*

[1]Department of Physics, Florida International University, Miami, FL 33199,
[2]Department of Chemistry and Biochemistry, The Eck Institute for Global Health and The Boler-Parseghian Center for Rare and Neglected Diseases, University of Notre Dame, Notre Dame, IN 46556,
[3]Biomolecular Sciences Institute, Florida International University, Miami, FL 33199,
[4]Department of Biochemistry and Molecular Biology, Indiana University School of Medicine-South Bend, South Bend, IN 46617.

[5]Current address: Department of Medicinal Chemistry and Molecular Pharmacology, Purdue University, West Lafayette, IN 47907.

Abstract

Ebola virus infections cause hemorrhagic fever that often results in very high fatality rates. In addition to exploring vaccines, development of drugs is also essential for treating the disease and preventing the spread of the infection. The Ebola virus matrix protein VP40 exists in various conformational and oligomeric forms and is a potential pharmacological target for disrupting the virus life-cycle. Here we explored graphene-VP40 interactions using molecular dynamics simulations and graphene pelleting assays. We found that graphene sheets associate strongly with VP40 at various interfaces. We also found that the graphene is able to disrupt the C-terminal domain (CTD-CTD) interface of VP40 hexamers. This VP40 hexamer-hexamer interface is crucial in forming the Ebola viral matrix and disruption of this interface may provide a method to use graphene or similar nanoparticle based solutions as a disinfectant that can significantly reduce the spread of the disease and prevent an Ebola epidemic.

*Corresponding Author
Email: chapagap@fiu.edu
Phone: +1 (305) 348 6266

This is the author's manuscript of the article published in final edited form as:

Gc, J. B., Pokhrel, R., Bhattarai, N., Johnson, K. A., Gerstman, B. S., Stahelin, R. V., & Chapagain, P. P. (2017). Graphene-VP40 interactions and potential disruption of the Ebola virus matrix filaments. Biochemical and Biophysical Research Communications. https://doi.org/10.1016/j.bbrc.2017.09.052

Introduction

Ebola virus (EBOV) infections are caused by a lipid-enveloped filovirus, which can cause hemorrhagic fever that often results in very high fatality rates [1]. The most recent outbreak in Western Africa in 2014 was the worst Ebola epidemic in history [2]. Although now essentially contained, this terrible outbreak has underscored the threat of new pandemics that could spread globally and kill tens of thousands of people [3]. Vaccine developments and small molecule identification are currently being pursued [4] but FDA approved drugs or vaccines are still lacking [5] [6]. A recent FDA study with an investigational Ebola vaccine has allowed identification of the vaccine-triggered antibodies as well as novel immune system targets, demonstrating great promise for new vaccine designs [7]. In addition to exploring vaccines, drug development may also be essential for treating the infection. For this, both the drug targets as well as the attacking small molecules need to be explored. The Ebola virus protein VP40 (eVP40) is a protein encoded by one of the seven genes that the Ebola virus carries. VP40 exists in various conformational and oligomeric states and is one of the potentially druggable Ebola proteins [8],[9]. The ability of VP40 to undergo conformational changes allows it to perform multiple functions[10],[11],[12] during the viral life-cycle[13]. Known conformational states of eVP40 include a butterfly shaped dimer that is involved in the transport of the protein to the membrane, a hexameric structure that is involved in forming the viral matrix, and an octamer ring structure that binds RNA and regulates viral transcription[13].

VP40 filaments constitute the major component of the viral matrix layer underneath the lipid envelope. The viral matrix provides the shape and stability of the virus particle and it has been shown that the expression of the VP40 protein in mammalian cells is sufficient for forming innocuous virus-like particles (VLPs)[14]. Following the hexamerization of the VP40 dimers at the cytosolic leaflet of the plasma membrane, filaments assemble through end-to-end interactions between the tail CTDs of the hexamers. The interfacial hydrophobic residues L203, I237, M241, M305, and I307 are suggested to be important in these interactions [13]. Specifically, mutagenesis studies have shown that VP40-M241R mutation causes obstruction in filament formation and results in defective membrane morphology of the budding VLPs. These results highlight the importance of CTD-CTD interfacial interactions in the Ebola virus life cycle. The

CTD interface involved in the hexamer-hexamer association can be a potential target for exploring small molecules that inhibit the formation of the viral matrix. Inspired by the studies that showed destruction of amyloid fibrils by graphene sheets [15], we sought to explore the graphene interactions with VP40 and the potential detrimental effects on the virus matrix.

Graphene sheets are composed of sp^2 hybridized conjugated carbon atoms and are one atom-thick [16]. Because of their mechanical stability, well-understood surface chemistry, and excellent optical and thermal properties, they are extensively studied for use in nanotechnology and are promising for a wide range of biomedical applications such as gene delivery, cellular imaging, and tumor therapy [17]. Many theoretical, experimental, and computational studies have explored the interaction of graphene sheets with cell membranes and proteins[18] [19] [20] [21] [22] [23] [24-26] [27, 28]. The molecular mechanism behind the antibacterial activity of graphene sheets on Escherichia coli was investigated with molecular dynamics (MD) simulations and experiments. It was found that the graphene treatment significantly reduced bacterial activity by disrupting the inner and outer cell membranes, highlighting the potential cytotoxicity and antibacterial properties of graphene sheets [27]. In another study, Luan et al. observed that graphene sheets can recognize and break hydrophobic protein-protein interactions in an HIV-1 integrase dimer [17]. Also, membrane disruption by graphene in healthy cells can hinder metabolism and cause cell death. Graphene oxide was found to be less toxic compared to pristine graphene sheets [29]. Combined molecular dynamics simulations and experimental studies showed inhibition of Aβ peptide amyloid fibrillization by graphene sheets, opening up the possibility of nanotherapy for Alzheimer's and protein-aggregation related diseases [13]. In another study, the nonporous graphene sheets were observed to desalinate a membrane [30]. Graphene sheets can also be used in membrane distillation and reverse osmosis [31]. Similarly, the adsorption mechanisms of serum proteins and graphene sheets were examined with experimental and molecular dynamics studies and it was found that both enthalpy and hydrophobic interactions contributed to the adsorption process [29].

We performed molecular dynamics simulations and graphene pelleting assays to explore the interactions between the Ebola matrix protein VP40 and graphene sheets. We explored whether graphene can insert into various interfaces in the VP40 filaments that make up the viral matrix. The CTD-CTD interface through which two hexamers connect end-to-end is a potential target as it features mostly hydrophobic residues. As such, experiments have highlighted the

importance of the hydrophobic residues L203, I237, M241, M305, and I307 in stabilizing the oligomerization interface [13]. We also investigated the dimer interface but found little penetration of the graphene. Our MD simulations of graphene interactions show that graphene sheets can insert through the matrix filament's CTD-CTD interfacial region connecting two hexamers and separate them. This suggests a potential antiviral activity of graphene. Graphene cytotoxicity can limit its use in nanotherapy to treat diseases directly. However, if graphene can break apart the viral matrix filaments and disrupt the virion, it can be used as a disinfectant that can significantly reduce the spread of the disease and prevent an Ebola epidemic.

2. Methods

Molecular Dynamics Simulations

The Ebola virus matrix is composed of filaments that are formed by VP40 hexamers connected end-to-end via their tail CTDs, as shown in Fig. 1. To use molecular dynamics simulations to investigate the ability of graphene to disrupt the structure of VP40 oligomers, VP40-graphene systems with no membrane were set-up with graphene placed close to various interfaces. The 30×40 $Å^2$ graphene sheet was built using the Carbon Nanostructure Builder Plugin in VMD [32]. The system for graphene insertion through the hexamer-hexamer interface (CTD-CTD) included just the two CTDs in order to lower the size of the system. This system consisted of 53,320 atoms in a periodic box of 85×99×67 $Å^3$. We ran three different simulations related to the hexamer CTD-CTD interface: the graphene sheet placed on the side of the interface that would face the cell membrane, the graphene sheet on the side opposite to the membrane that faces the inside of the cell, and a control simulation of the CTD-CTD complex without the graphene. Similar systems were set up for the graphene insertion through the dimer interface. All MD simulations were performed using NAMD 2.11 [33] with the CHARMM36 force field [34]. Periodic boundary conditions were employed in all simulations. The long range electrostatic interactions were treated using the particle mesh Ewald (PME) method [35]. To constrain the covalent bonds involving hydrogen atoms, the SHAKE algorithm [36] was used. Minimization of the system was followed by the production run. The simulation time step was set to 2 fs for all productions runs. A Nose-Hoover Langevin-piston [37] method was used with a piston period of 50 fs and a decay of 25 fs to control the pressure. The temperature was controlled using Langevin temperature coupling with a friction coefficient of 1 ps^{-1}.

For calculations of hydrogen bonds, the cut-off distance and cut-off angle were 3.5 Å and 30^o respectively. The calculation of the time-evolving surface contact area between CTDs as they separate from each other used the following:

$$Contact\ Area = \frac{S_{C1} + S_{C2} - S_{C1C2}}{2} \quad (1)$$

where S_{C1} and S_{C2} represent the solvent accessible surface areas of the individual CTDs labelled as C1 and C2 respectively, and S_{C1C2} is the solvent accessible surface area of C1 and C2 taken together. The solvent accessible area of graphene and the CTDs ($S_{C1\text{-}GRA}$ and $S_{C2\text{-}GRA}$ respectively) were also calculated in a similar manner.

Experiments

Protein Expression and Purification:

Full length 6xHis-VP40 in pET46 was transformed into Rosetta BL21 DE3 cells (Novagen, Madison, Wisconsin). One colony was picked from the transformation plate and grown at 37°C at 200 rpm until an OD_{600} of 0.4-0.6. VP40 expression was induced with 1 mM IPTG for 5 hours at room temperature. Protein was purified using a Ni NTA affinity resin (Thermo Scientific, Waltham, MA). Eluted protein was further purified using size exclusion chromatography (HiLoad 16/600 Superdex 200 pg column on an AKTA Prime Plus system (GE Healthcare Life Sciences, Pittsburgh, PA)) to separate the VP40 dimer and oligomer. VP40 dimer protein was concentrated and stored in 10 mM Tris, pH 8.0 containing 300 mM NaCl. Protein concentration was determined with a Pierce BCA Protein Assay Kit according to the manufacturer's instructions (Thermo Scientific).

Graphene Pelleting Assay

Nano Graphene Oxide Solution (GO), 125 ml (1g/L) was purchased from Graphene Supermarket (Calverton, NY). 1 mL GO solution was pelleted through centrifugation (16,873 rcf for 10 minutes), the supernatant was removed and the pellet was resuspended in reaction buffer (10 mM Tris, 150 mM NaCl). 2 μM VP40 was prepared without GO or with 0.2 mg or 1.0 mg GO in a 200 uL reaction for 30 minutes at room temperature. After this time, the solution

was centrifuged to pellet the GO. The top 180 uL of the supernatant was removed and the pellet was resuspended in 160 uL for a total of 180 uL. Samples were run on SDS PAGE to visualize protein localization. ImageJ was used to determine the protein band density from each sample supernatant (SN) and pellet (P).

3. Results

Characteristics of the CTD-CTD Oligomerization Interface:

The oligomerization interface that connects two hexamers end-to-end occurs via tail CTDs, as shown in Fig. 1. Figure 1 shows that at the interface, the CTD from one hexamer is inverted compared to the CTD from the other hexamer. The CTD interface contains hydrophobic residues L203, I237, M241, M305, and I307 that stabilize the interface. These CTD-CTD interactions are a critical part of the Ebola virus matrix structure [38]. For example, an M241R mutation results in the disruption of VP40 filaments and hinders virus budding [13]. The non-specific hydrophobic interactions at this hexamer CTD-CTD interface are thought to provide flexibility to the filaments, which can explain the pleomorphic nature of the filovirus virion [13] [39] [40]. Therefore, without the graphene insertion, this CTD-CTD interface is flexible but stable.

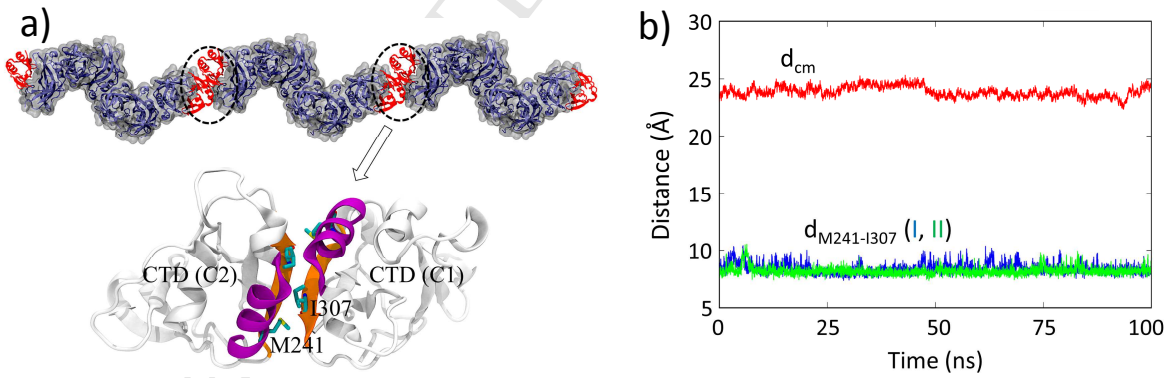

Figure 1. a) A section of an Ebola virus VP40 filament composed of three hexamers connected end-to-end via tail CTDs. The CTD-CTD oligomerization interface is highlighted in red. Hydrophobic residues (M241 and I307) stabilizing the hexamer-hexamer oligomerization interface are highlighted. b) The time evolution of the center of mass distance between the two

CTDs, and the C_α-C_α distance between the two residue pairs of M241 and I307 from the MD simulation of the hexamer CTD interface without a graphene sheet showing the stability of the interface.

As a control, we first performed a 100-ns MD simulation of the interface CTDs without graphene. Figure 1 illustrates the time evolution of the center of mass distance (d_{cm}) between the two CTDs C1 and C2 (Fig. 1), as well as the C_α-C_α distance between the important residues of M241 from one hexamer and I307 from the other hexamer. Since each CTD contains the same residues, there are two pairs of M241-I307 distances, and Fig. 1b includes plots for both pairs. The center of mass distance between the two CTDs remains slightly below 25 Å throughout the simulation, showing that the interface is quite stable. Similarly, the C_α-C_α distance between M241 and I307 also remains stable at ~ 8 Å. In addition to the hydrophobic interactions, the CTD interface has a few hydrogen bonds. As with d_{cm} and $d_{M241\text{-}I307}$ distances, in this same MD simulation without graphene, there were no significant changes in the number of the interfacial contacts and hydrogen bonds.

Graphene Insertion through the CTD-CTD interface

To explore the graphene-VP40 interaction and possible insertion of the graphene through the oligomerization interface, we performed MD simulations of the CTDs with graphene placed slightly above the interface on the side that would face the cell membrane, as shown in Fig. 2a. The hydrophobic core formed by the important stabilizing residues M241 and I307 is buried deep in the interface and not exposed to graphene at the beginning of the simulation. Therefore, the graphene sheet has to first make its way through the initial contacts of A229 and P234 before it can break the important hydrophobic contacts between M241 and I307. With the highly hydrophobic nature of graphene, it is entropically driven towards making contacts with the protein, mostly the hydrophobic residues, but basic as well as aromatic residues are also known to interact strongly with graphene [41]. Indeed, with the right orientation, the graphene sheet is found to insert through A229/P234 contacts relatively easily, but further insertion is hindered by the strong hydrophobic core (Fig. 2b).

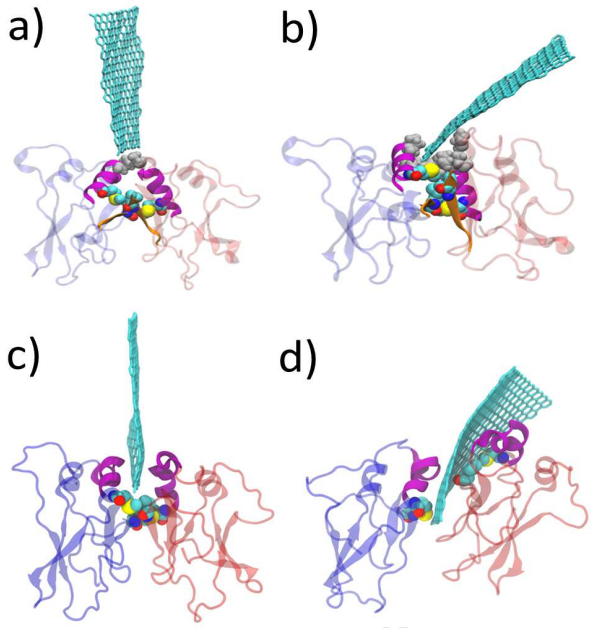

Fig. 2. MD snapshots of the graphene insertion through the hexamer CTD-CTD interface. a-b) Initial breaking of A229/P234 and c-d) graphene disrupting the M241-I307 pair and inserting farther into the interface.

Since the rate-limiting step is to break the hydrophobic core involving residues M241 and I307, we started new simulations from the conformation in Fig. 2c in which the graphene sheet is already past A229/P234 but not in the M241/I307 core. Vertical reorientation of the graphene sheet at this conformation can expedite the insertion process to complete in a reasonable computational time. Figure 2c shows the initial graphene-protein complex in which the graphene is within 3.5 Å of the first M241-I307 pair. The M241/I307 core is found to remain intact for another 120 ns, after which the graphene is able to disrupt this pair and insert farther into the interface (Fig. 2d)

As the graphene sheet is inserted through the CTDs interface, the center of mass distance between the two CTDs increases by 5 Å as shown in Fig. 3a (C1-C2 curve). The center of mass distance between C1 and graphene decreases by ~5 Å, whereas the distance between C2 and graphene decreases by ~15 Å. As shown in Fig. 3b, both pairs of the hydrophobic residue interactions between M241-I307 that stabilize the CTD-interface were broken after 120 ns. These two pairs of hydrophobic residues are labeled as I and II in Fig. 3b as was done in Fig. 1b.

As these residues move farther apart, the contact area between the CTDs decreases (Fig. 3c, red curve) from 400 $Å^2$ to below 100 $Å^2$, whereas the contact areas between the graphene and the CTDs increases. In general, the CTD C2 is found to have more robust contacts with the graphene compared to C1 (blue curve graphene-C2 ~1400 $Å^2$ vs. green curve graphene-C1 ~600 $Å^2$). This is also displayed by the van der Waals (VDW) contact energy between the CTDs and graphene (Fig. 3d).

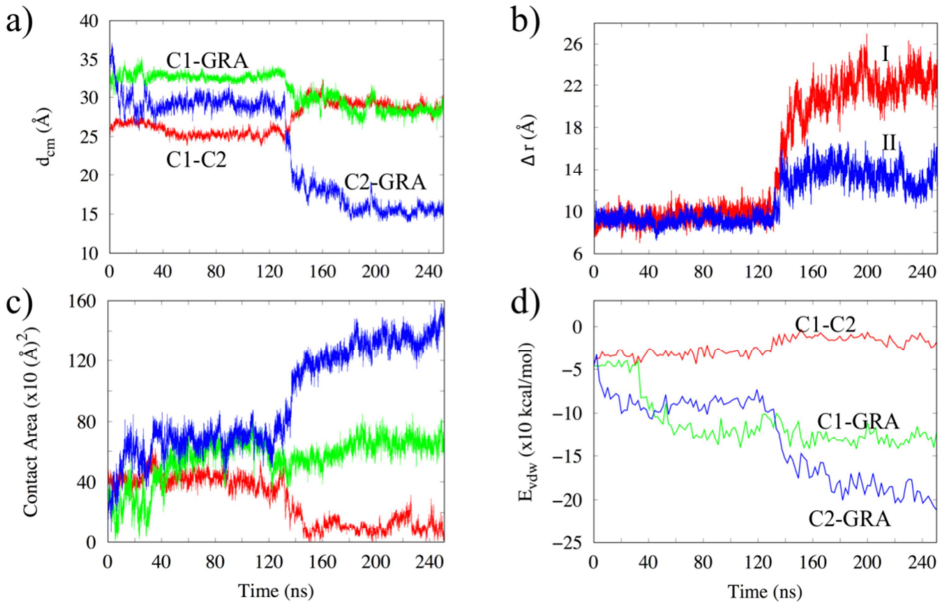

Fig. 3. Time evolution of various structural/energy parameters during the graphene sheet insertion. a) Center of mass distance between the two CTDs (C1-C2), C1-graphene (C1-GRA) and C2-graphene (C2-GRA). b) Distance between the hydrophobic residues M241-I307 (pair I and pair II). c) Contact area between C1, C2, and graphene (same color scheme as in a). d) van der Waals (VDW) interaction energies between the CTDs and the graphene sheet.

By 150 ns of MD simulation, the graphene is able to fully insert through the CTD-CTD interface. Figure 4a shows the amino acid residues that are in contact with the graphene sheet before and after the CTD-CTD interface separation. In addition to hydrophobic residues, polar and charged residues are also found to interact with the graphene sheet. We also monitored if the CTD-graphene interactions as the graphene inserts into the CTD-CTD interface affects the CTD secondary structure. Several recent studies have shown that protein-graphene interactions can

lead to secondary structural changes [26]. For example, an HIV-1 regulatory protein undergoes α-helix to β-sheet structural changes upon graphene association [18]. Similarly, VPR_{13-33} adsorption on the graphene oxide surface caused the loss of secondary structure [42]. Strong dispersion interactions of the solvent-exposed basic residues and graphene can provide the major driving force [41] for protein structural changes. In our MD simulations, we did not observe any significant secondary structural changes of the CTD interacting with the graphene.

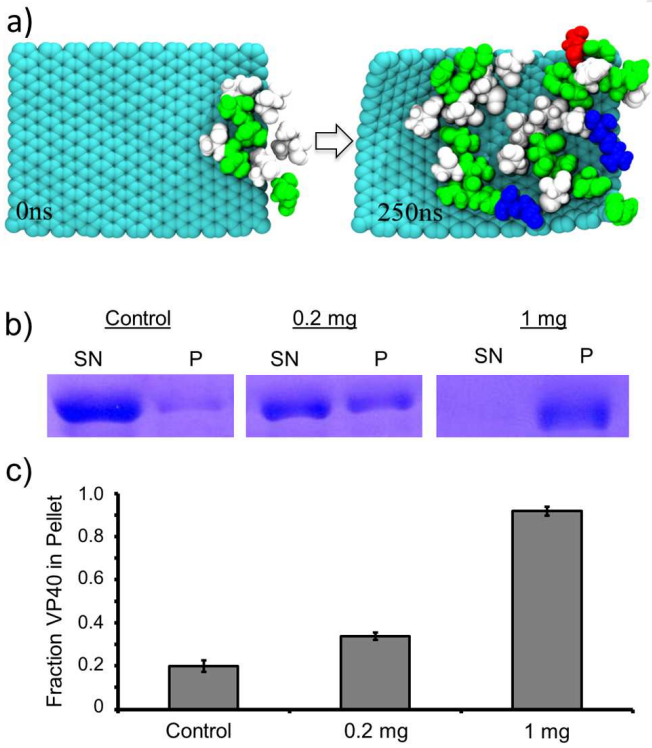

Fig. 4: a) Amino acid residues within 3.5 Å of graphene at 0 ns and 250 ns (white-hydrophobic, green-polar, blue-basic, red-acidic) b) Representative images of SDS PAGE of VP40 protein in the supernatant (SN) or pellet (P) fractions of the sample without and with 0.2 mg or 1 mg graphene. c) Quantification of VP40 in the pellet fraction for each condition. Error bars are +/- standard error of the mean. Data represents three independent experiments with three replicates per experiment.

Graphene-VP40 Interactions at other interfaces

We also performed MD simulations to investigate if graphene can insert into other interfaces. In one simulation, we placed the graphene close to the same CTD hexamer interface

investigated above, but on the other side that would face the inside of the cell. In another simulation, we placed the graphene sheet close to the NTD-NTD interface in the VP40 dimer. In neither of these simulations did the graphene sheet insert into the interface. However, a strong association of VP40 with graphene is observed in all simulations, giving various forms of graphene-VP40 complexes. In order to confirm the formation of graphene-VP40 complexes, we performed a graphene pelleting assay with concentrated VP40 dimers and graphene oxide solution. In solution, graphene is easily pelleted with centrifugation but VP40 pellets weakly (Fig. 4b and c, Control unless bound to graphene. As shown in Fig. 4b, a significant protein band density is observed in the pellet (P) only when VP40 is co-incubated with graphene oxide. We quantified the VP40 in the pellet fraction for each condition as displayed in Fig. 4c and found that VP40 pelleting increases with increasing graphene oxide concentrations. When 1mg graphene is added, nearly all VP40 is bound to graphene oxide and observed in the pellet. These results show that graphene indeed associates strongly with VP40.

Conclusion

We investigated graphene-VP40 interactions using molecular dynamics simulations and graphene pelleting assays. We found that graphene sheets associate strongly with Ebola VP40 oligomers. Similar to the observations in the HIV-1 integrase dimer[17] and Aβ amyloid fibrils [13], we found that graphene sheets can recognize and break hydrophobic protein-protein interactions in the Ebola matrix protein VP40. The graphene is able to insert through the CTD-CTD interface connecting VP40 hexamers. This VP40 hexamer-hexamer oligomerization interface is crucial in forming the VP40 filaments that make up the Ebola virus matrix and breaking of the interface provides a method to disrupt the viral matrix. As with graphene's antibacterial activity of disrupting the inner and outer cell membranes, further experiments are needed to confirm the potential antiviral activity of graphene in Ebola virus. Though graphene cytotoxicity can limit its use in nanotherapy to treat diseases directly, if graphene can break apart the viral matrix filaments and disrupt the virion, its antiviral activity can be exploited in disinfecting surfaces harboring the mature virions which can significantly reduce the spread of the disease and prevent an Ebola epidemic.

Acknowledgements

VP40 research has been supported by the NIH (AI081077) to R.V.S.

References

[1] J.H. Kuhn, S. Becker, H. Ebihara, T.W. Geisbert, K.M. Johnson, Y. Kawaoka, W.I. Lipkin, A.I. Negredo, S.V. Netesov, S.T. Nichol, G. Palacios, C.J. Peters, A. Tenorio, V.E. Volchkov, P.B. Jahrling, Proposal for a revised taxonomy of the family Filoviridae: classification, names of taxa and viruses, and virus abbreviations, Arch Virol, 155 (2010) 2083-2103.
[2] E. Cox, L. Borio, R. Temple, Evaluating Ebola therapies--the case for RCTs, N Engl J Med, 371 (2014) 2350-2351.
[3] E. Tambo, C.F. Chengho, C.E. Ugwu, I. Wurie, J.K. Jonhson, J.Y. Ngogang, Rebuilding transformation strategies in post-Ebola epidemics in Africa, Infect Dis Poverty, 6 (2017) 71.
[4] A.R. Menicucci, S. Sureshchandra, A. Marzi, H. Feldmann, I. Messaoudi, Transcriptomic analysis reveals a previously unknown role for CD8+ T-cells in rVSV-EBOV mediated protection, Sci Rep, 7 (2017) 919.
[5] N.J. Sullivan, J.E. Martin, B.S. Graham, G.J. Nabel, Correlates of protective immunity for Ebola vaccines: implications for regulatory approval by the animal rule, Nat Rev Micro, 7 (2009) 393-400.
[6] H. Feldmann, T.W. Geisbert, Ebola haemorrhagic fever, Lancet, 377 (2011) 849-862.
[7] S. Khurana, S. Fuentes, E.M. Coyle, S. Ravichandran, R.T. Davey, Jr., J.H. Beigel, Human antibody repertoire after VSV-Ebola vaccination identifies novel targets and virus-neutralizing IgM antibodies, Nat Med, 22 (2016) 1439-1447.
[8] R.V. Stahelin, Could the Ebola virus matrix protein VP40 be a drug target?, Expert Opin Ther Targets, 18 (2014) 115-120.
[9] J.J. Madara, Z. Han, G. Ruthel, B.D. Freedman, R.N. Harty, The multifunctional Ebola virus VP40 matrix protein is a promising therapeutic target, Future Virol, 10 (2015) 537-546.
[10] N. Tokuriki, D.S. Tawfik, Protein dynamism and evolvability, Science, 324 (2009) 203-207.
[11] P. Tompa, C. Szasz, L. Buday, Structural disorder throws new light on moonlighting, Trends Biochem Sci, 30 (2005) 484-489.
[12] J.B. Gc, B.S. Gerstman, P.P. Chapagain, The Role of the Interdomain Interactions on RfaH Dynamics and Conformational Transformation, The journal of physical chemistry. B, 119 (2015) 12750-12759.
[13] Z.A. Bornholdt, T. Noda, D.M. Abelson, P. Halfmann, M.R. Wood, Y. Kawaoka, E.O. Saphire, Structural rearrangement of ebola virus VP40 begets multiple functions in the virus life cycle, Cell, 154 (2013) 763-774.
[14] L.D. Jasenosky, G. Neumann, I. Lukashevich, Y. Kawaoka, Ebola virus VP40-induced particle formation and association with the lipid bilayer, J Virol, 75 (2001) 5205-5214.
[15] Z. Yang, C. Ge, J. Liu, Y. Chong, Z. Gu, C.A. Jimenez-Cruz, Z. Chai, R. Zhou, Destruction of amyloid fibrils by graphene through penetration and extraction of peptides, Nanoscale, 7 (2015) 18725-18737.
[16] F. De Leo, A. Magistrato, D. Bonifazi, Interfacing proteins with graphitic nanomaterials: from spontaneous attraction to tailored assemblies, Chem Soc Rev, 44 (2015) 6916-6953.
[17] B. Luan, T. Huynh, L. Zhao, R. Zhou, Potential toxicity of graphene to cell functions via disrupting protein-protein interactions, ACS Nano, 9 (2015) 663-669.
[18] D. Zhao, L. Li, D. He, J. Zhou, Molecular dynamics simulations of conformation changes of HIV-1 regulatory protein on graphene, Applied Surface Science, 377 (2016) 324-334.

[19] M. Dallavalle, M. Calvaresi, A. Bottoni, M. Melle-Franco, F. Zerbetto, Graphene can wreak havoc with cell membranes, ACS Appl Mater Interfaces, 7 (2015) 4406-4414.
[20] N. Dragneva, O. Rubel, W.B. Floriano, Molecular Dynamics of Fibrinogen Adsorption onto Graphene, but Not onto Poly(ethylene glycol) Surface, Increases Exposure of Recognition Sites That Trigger Immune Response, J Chem Inf Model, 56 (2016) 706-720.
[21] A.V. Titov, P. Kral, R. Pearson, Sandwiched graphene--membrane superstructures, ACS Nano, 4 (2010) 229-234.
[22] X. Zou, L. Zhang, Z. Wang, Y. Luo, Mechanisms of the Antimicrobial Activities of Graphene Materials, J Am Chem Soc, 138 (2016) 2064-2077.
[23] J. Chen, G. Zhou, L. Chen, Y. Wang, X. Wang, S. Zeng, Interaction of Graphene and its Oxide with Lipid Membrane: A Molecular Dynamics Simulation Study, The Journal of Physical Chemistry C, 120 (2016) 6225-6231.
[24] J. Mao, R. Guo, L.T. Yan, Simulation and analysis of cellular internalization pathways and membrane perturbation for graphene nanosheets, Biomaterials, 35 (2014) 6069-6077.
[25] M. Feng, H. Kang, Z. Yang, B. Luan, R. Zhou, Potential disruption of protein-protein interactions by graphene oxide, J Chem Phys, 144 (2016) 225102.
[26] L. Baweja, K. Balamurugan, V. Subramanian, A. Dhawan, Effect of graphene oxide on the conformational transitions of amyloid beta peptide: A molecular dynamics simulation study, J Mol Graph Model, 61 (2015) 175-185.
[27] Y. Tu, M. Lv, P. Xiu, T. Huynh, M. Zhang, M. Castelli, Z. Liu, Q. Huang, C. Fan, H. Fang, R. Zhou, Destructive extraction of phospholipids from Escherichia coli membranes by graphene nanosheets, Nat Nanotechnol, 8 (2013) 594-601.
[28] B. Zhang, P. Wei, Z. Zhou, T. Wei, Interactions of graphene with mammalian cells: Molecular mechanisms and biomedical insights, Adv Drug Deliv Rev, 105 (2016) 145-162.
[29] Y. Chong, C. Ge, Z. Yang, J.A. Garate, Z. Gu, J.K. Weber, J. Liu, R. Zhou, Reduced Cytotoxicity of Graphene Nanosheets Mediated by Blood-Protein Coating, ACS Nano, 9 (2015) 5713-5724.
[30] G. Hummer, J.C. Rasaiah, J.P. Noworyta, Water conduction through the hydrophobic channel of a carbon nanotube, Nature, 414 (2001) 188-190.
[31] D. Cohen-Tanugi, L.C. Lin, J.C. Grossman, Multilayer Nanoporous Graphene Membranes for Water Desalination, Nano Lett, 16 (2016) 1027-1033.
[32] W. Humphrey, A. Dalke, K. Schulten, VMD: visual molecular dynamics, J Mol Graph, 14 (1996) 33-38, 27-38.
[33] J.C. Phillips, R. Braun, W. Wang, J. Gumbart, E. Tajkhorshid, E. Villa, C. Chipot, R.D. Skeel, L. Kalé, K. Schulten, Scalable molecular dynamics with NAMD, Journal of Computational Chemistry, 26 (2005) 1781-1802.
[34] A.D. Mackerell, Jr., Empirical force fields for biological macromolecules: overview and issues, J Comput Chem, 25 (2004) 1584-1604.
[35] U. Essmann, L. Perera, M.L. Berkowitz, T. Darden, H. Lee, L.G. Pedersen, A Smooth Particle Mesh Ewald Method, Journal of Chemical Physics, 103 (1995) 8577-8593.
[36] J.-P. Ryckaert, G. Ciccotti, H.J. Berendsen, Numerical integration of the cartesian equations of motion of a system with constraints: molecular dynamics of n-alkanes, Journal of Computational Physics, 23 (1977) 327-341.
[37] M.M. Brooks, A. Hallstrom, M. Peckova, A simulation study used to design the sequential monitoring plan for a clinical trial, Stat Med, 14 (1995) 2227-2237.

[38] J. Timmins, S. Scianimanico, G. Schoehn, W. Weissenhorn, Vesicular release of ebola virus matrix protein VP40, Virology, 283 (2001) 1-6.
[39] D.R. Beniac, P.L. Melito, S.L. Devarennes, S.L. Hiebert, M.J. Rabb, L.L. Lamboo, S.M. Jones, T.F. Booth, The organisation of Ebola virus reveals a capacity for extensive, modular polyploidy, PLoS One, 7 (2012) e29608.
[40] T.A. Bharat, T. Noda, J.D. Riches, V. Kraehling, L. Kolesnikova, S. Becker, Y. Kawaoka, J.A. Briggs, Structural dissection of Ebola virus and its assembly determinants using cryo-electron tomography, Proc Natl Acad Sci U S A, 109 (2012) 4275-4280.
[41] Z. Gu, Z. Yang, L. Wang, H. Zhou, C.A. Jimenez-Cruz, R. Zhou, The role of basic residues in the adsorption of blood proteins onto the graphene surface, Sci Rep, 5 (2015) 10873.
[42] S. Zeng, G. Zhou, J. Guo, F. Zhou, J. Chen, Molecular simulations of conformation change and aggregation of HIV-1 Vpr13-33 on graphene oxide, Scientific Reports, 6 (2016) 24906.

Research Highlights

- VP40-graphene interactions were explored using molecular dynamics simulations
- Graphene sheet was found to insert through the hexamer-hexamer C-terminal interface
- Potential destruction of the viral matrix with graphene nanosheets is discussed